

A comparative analysis of kinetically consistent schemes with several grid methods for solving gas-dynamics problems*

G.G. Lazareva, A.G. Maksimova

Abstract. The equations of gas dynamics are an integral part of numerical models of the atmospheric dynamics used for research into variations of climate and anthropogenic changes in the environment. Various modifications of the discrete kinetic models describing a single-particle distribution function are reviewed and tested. A comparison of test solutions with the explicit solutions is made. A counterexample showing the necessity of considering the sequence of derivation of equations is given.

1. Kinetically consistent difference schemes

Let us consider a non-trivial approach to the creation of computational algorithms for solving the gas dynamics equations. At first, the difference approximation of the Boltzmann equation is constructed [1] to create kinetically consistent difference schemes (KCDS). Then, this approximation is averaged in the velocity of molecules, and difference equations for the gas dynamics parameters are derived. In the conventional methods of solving the gas dynamics equations, the sequence of actions is different. At first, the Boltzmann equation is averaged in the velocity of molecules using assumptions about the distribution function and the Navier–Stokes or the Euler equations are obtained. Only after that, a difference approximation is constructed.

This approach is originated on the following assumptions [2]. At the moment of time t^n , the one-particle distribution function is a constant at every segment $[x_j, x_{j+1}]$ and coincides with the Maxwell one. The gas dynamics parameters ρ_j , u_j , p_j are also stable at every segment $[x_j, x_{j+1}]$. During time $\tau = t^{n+1} - t^n$ the gas makes a collisionless expansion. At every moment t^n , an instant maxwellization of the distribution function takes place. Note that the one-particle Maxwell distribution function is adequate for gas dynamics processes and corresponds to the collisions of molecules in the gas. In this approach, the cumbersome scheme with the error integral arising after averaging in speed is obtained:

*Supported by the RAS Presidium Program 17.5 “Intellectual information technologies and systems.”

$$\begin{aligned}
\frac{\rho_i^{n+1} - \rho_i^n}{\tau} + (\rho u)_{\dot{x}} &= \frac{h}{2} \left[\rho u \operatorname{erf}(s) + \frac{1}{\beta \sqrt{\pi}} \exp(-s^2) \right]_{\bar{x}x}, \\
\frac{(\rho u)_i^{n+1} - (\rho u)_i^n}{\tau} + (\rho u^2 + p)_{\dot{x}} &= \frac{h}{2} \left[(\rho u^2 + p) \operatorname{erf}(s) + \frac{\rho u \exp(-s^2)}{\beta \sqrt{\pi}} \right]_{\bar{x}x}, \quad (1) \\
\frac{E_i^{n+1} - E_i^n}{\tau} + (u(E+p))_{\dot{x}} &= \frac{h}{2} \left[u(E+p) \operatorname{erf}(s) + \frac{1}{\beta \sqrt{\pi}} \left(E + \frac{p}{2} \right) \exp(-s^2) \right]_{\bar{x}x},
\end{aligned}$$

where ρ is gas density, h is the spatial step, T is the temperature, $p = \rho RT$ is the gas pressure, u is the gas velocity, γ is the adiabatic index, $\varepsilon = \frac{RT}{\gamma - 1}$ is the internal energy, $E = \frac{\rho u^2}{2} + \rho \varepsilon$ is the full energy. The error integral is $\operatorname{erf}(s) = \frac{2}{\sqrt{\pi}} \int_0^s \exp(-z^2) dz$, where $s = \beta u$, $\beta = \frac{1}{\sqrt{2RT}}$. For the approximation of the first derivative, the central difference $a_{\dot{x}} = \frac{a_{i+1} - a_{i-1}}{2h}$ is used. For the approximation of the second derivative, the difference approximation $a_{\bar{x}x} = \frac{a_{i+1} - 2a_i + a_{i-1}}{2h^2}$ is applied.

A quasi-gasdynamics system of equations

A quasi-gasdynamics system of equations (QGS) is one of the forms of KCDS differential recording [3]. The QGS is often used as the basis of computational algorithms due to its relative simplicity:

$$\begin{aligned}
\frac{\rho_i^{n+1} - \rho_i^n}{\tau} + (\rho u)_{\dot{x}} &= \tau_c (\rho u^2 + p)_{\bar{x}x}, \\
\frac{(\rho u)_i^{n+1} - (\rho u)_i^n}{\tau} + (\rho u^2 + p)_{\dot{x}} &= \tau_c (\rho u^3 + 3pu)_{\bar{x}x}, \quad (2) \\
\frac{E_i^{n+1} - E_i^n}{\tau} + (u(E+p))_{\dot{x}} &= \tau_c (u^2(E+2p))_{\bar{x}x} + \tau_c \left(\frac{p}{\rho} (E+p) \right)_{\bar{x}x},
\end{aligned}$$

where $\tau_c \approx \frac{h}{2c}$ is the kinetic time during which molecules cross the cell boundaries. Note that the system of gas dynamics equations is of the hyperbolic type, and the QGS is of the parabolic type [4].

The upwind scheme

We consider the first-order upwind scheme [5] on a uniform grid with different versions of the right-hand-side function $F = (f_1, f_2, f_3)^T$:

$$\begin{aligned}
& \frac{\rho_i^{n+1} - \rho_i^n}{\tau} + u_i^{n+} \frac{\rho_i^n - \rho_{i-1}^n}{h} + u_i^{n-} \frac{\rho_{i+1}^n - \rho_i^n}{h} + \rho_i^n \frac{u_{i+1}^n - u_{i-1}^n}{2h} = f_1, \\
& \frac{(\rho u)_i^{n+1} - (\rho u)_i^n}{\tau} + u_i^{n+} \frac{(\rho u)_i^n - (\rho u)_{i-1}^n}{h} + u_i^{n-} \frac{(\rho u)_{i+1}^n - (\rho u)_i^n}{h} + \\
& \quad (\rho u)_i^n \frac{u_{i+1}^n - u_{i-1}^n}{2h} + \frac{p_{i+1}^n - p_{i-1}^n}{2h} = f_2, \\
& \frac{E_i^{n+1} - E_i^n}{\tau} + u_i^{n+} \frac{E_i^n - E_{i-1}^n}{h} + u_i^{n-} \frac{E_{i+1}^n - E_i^n}{h} + E_i^n \frac{u_{i+1}^n - u_{i-1}^n}{2h} + \\
& \quad \frac{u_{i+1}^n p_{i+1}^n - u_{i-1}^n p_{i-1}^n}{2h} = f_3,
\end{aligned} \tag{3}$$

where $u_i^{n\pm} = \frac{u_i^n \pm |u_i^n|}{2}$, h and τ are spatial and temporal steps, respectively.

The right-hand side $F = (0, 0, 0)^T$ defines the upwind-leap-frog scheme.

The upwind scheme right-hand side for KCDS (1) is the following:

$$F = \begin{pmatrix} \frac{h}{2} \left[\rho u \operatorname{erf}(s) + \frac{1}{\beta\sqrt{\pi}} \exp(-s^2) \right]_{\bar{x}x} \\ \frac{h}{2} \left[(\rho u^2 + p) \operatorname{erf}(s) + \frac{\rho u \exp(-s^2)}{\beta\sqrt{\pi}} \right]_{\bar{x}x} \\ \frac{h}{2} \left[u(E + p) \operatorname{erf}(s) + \frac{1}{\beta\sqrt{\pi}} \left(E + \frac{p}{2} \right) \exp(-s^2) \right]_{\bar{x}x} \end{pmatrix} \tag{4}$$

The upwind scheme right-hand side for QGS (2) is the following:

$$F = \begin{pmatrix} \tau_c (\rho u^2 + p)_{\bar{x}x} \\ \tau_c (\rho u^3 + 3pu)_{\bar{x}x} \\ \tau_c (u^2(E + 2p))_{\bar{x}x} + \tau_c \left(\frac{p}{\rho} (E + p) \right)_{\bar{x}x} \end{pmatrix} \tag{5}$$

The Steger–Warming scheme

Similarly, we consider the Steger–Warming scheme [6] with three versions of the right-hand side:

$$\frac{U_i^{n+1} - U_i^n}{\tau} + \frac{F_{j+1/2}^n - F_{j-1/2}^n}{h} = 0, \tag{6}$$

where

$$\begin{aligned}
U &= (\rho, \rho u, E)^T, \quad F_{j+1/2} = A_j^+ U_j + A_{j+1}^- U_{j+1}, \\
A^\pm &= R D^\pm L, \quad D^\pm = \operatorname{diag}(d_1^\pm, d_2^\pm, d_3^\pm), \\
d_k^\pm &= \frac{1}{2}(a_k \pm |a_k|), \quad a_1 = u - c, \quad a_2 = u, \quad a_3 = u + c, \\
E &= \frac{\rho u^2}{2} + \frac{p}{\gamma - 1}, \quad c = \sqrt{\frac{\gamma p}{\rho}}, \quad H = \frac{E + p}{\rho},
\end{aligned}$$

$$L = \begin{pmatrix} uc + (\gamma - 1)\frac{u^2}{2} & -c - (\gamma - 1)u & \gamma - 1 \\ 1 - (\gamma - 1)\frac{u^2}{2c^2} & (\gamma - 1)\frac{u}{c^2} & -(\gamma - 1)\frac{1}{c^2} \\ -uc + (\gamma - 1)\frac{u^2}{2} & c - (\gamma - 1)u & \gamma - 1 \end{pmatrix},$$

$$R = L^{-1} = \begin{pmatrix} \frac{1}{2c^2} & 1 & \frac{1}{2c^2} \\ \frac{1}{2c^2}(u - c) & u & \frac{1}{2c^2}(u + c) \\ \frac{1}{2c^2}(H - uc) & \frac{u^2}{2} & \frac{1}{2c^2}(H + uc) \end{pmatrix}.$$

Here $F = (0, 0, 0)^T$ defines the Steger–Warming scheme, $F = (f_1, f_2, f_3)^T$ from (4) and (5) define the Steger–Warming scheme for KCDS (1) and QGS (2).

The test results

The Riemann problem has a known exact solution [7]. Let us consider the one-dimensional inviscid gas in the tube. Let a point $x = x_0$ be a damper that separates the gas in the tube. Gas on the left of the damper has the parameters ρ_1, u_1, p_1 and on the right of the damper — ρ_2, u_2, p_2 . For definiteness, we consider that $p_1 > p_2$. At the time $t = 0$, the damper is removed.

The initial data: $\rho_1 = 1, u_1 = 0, p_1 = 1, \rho_2 = 0.125, u_2 = 0, p_2 = 0.1$. We have made some tests showing the error density for different temporal and spatial steps at the time moment $t = 1$.

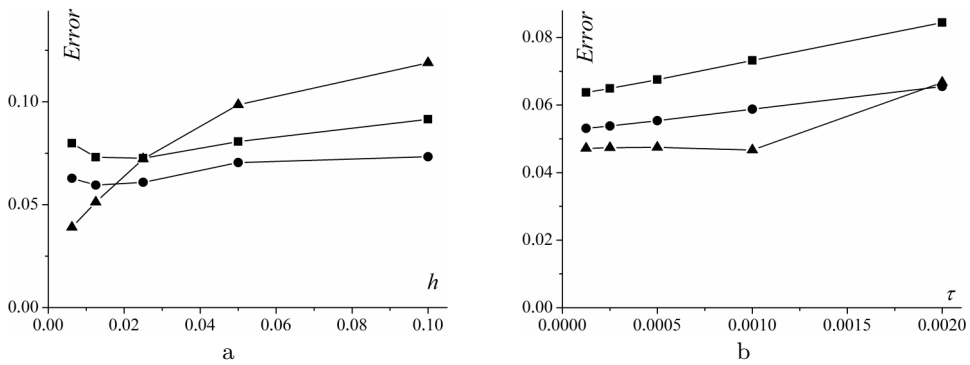


Figure 1. The error in the mean-square norm of the density calculation by the upwind scheme (the square symbol), with KCDS (the circle symbol), and with QGS (the triangle symbol): (a) different spatial steps, $\tau = 0.001$; (b) different temporal steps, $h = 0.01$

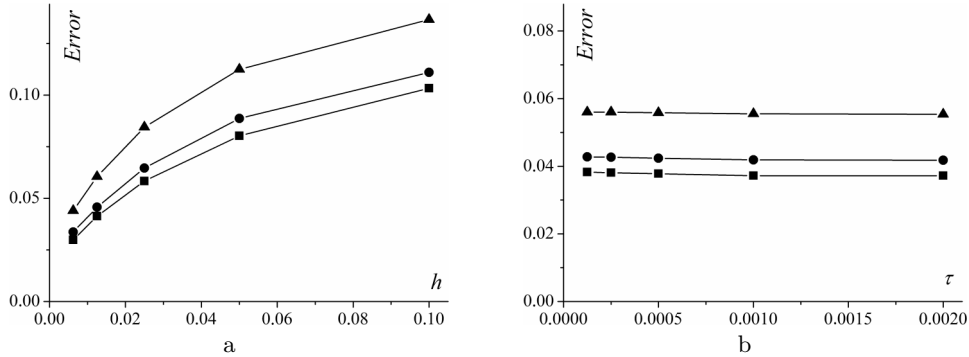


Figure 2. The error in the mean-square norm of the density calculation by the Steger–Warming scheme (the square symbol), with KCDS (the circle symbol), and with QGS (the triangle symbol): (a) different spatial steps, $\tau = 0.001$; (b) different temporal steps, $h = 0.01$

Graph in Figure 1 show that the scheme with KCDS is more accurate than the original upwind scheme (3). The scheme with QGS has advantages for small spatial steps and requires improving the order of convergence with respect to time. Note that the QGS of the second order of convergence with respect to time with an addition of the second temporal derivative returns the parabolic type of the solved system of equations [4].

Graphs in Figure 2 show that applying the right-hand side F from (4), (5) lowers the accuracy of the original Steger–Warming scheme (6). This is because the Steger–Warming scheme is a convective transport of gas-dynamics quantities in characteristics. This approach is not consistent with the construction method of KCDS and QGS. This counterexample provides a method of developing discrete kinetic models through the improvement of the approximation of the transfer in the Boltzmann equation.

The experimental analysis of the rate of the convergence for the dispersion of a sampling was carried out. The order of accuracy $\mathcal{P}(h)$ is determined for a certain value of f considering the sequential reduction of step h and using the Runge rule [8]:

$$\mathcal{P}(h) = \lim_{h \rightarrow 0} \log_2 \frac{f(2h) - f(h)}{f(h) - f(h/2)}.$$

Graphs in Figure 3 show that the rate of convergence doesn't have the first order of accuracy on the example of the law of conservation of mass:

$$f_\rho = \int_{x_1}^{x_2} \rho(x, t_2) dx - \int_{x_1}^{x_2} \rho(x, t_1) dx + \int_{t_1}^{t_2} (\rho u)(x_2, t) dt - \int_{t_1}^{t_2} (\rho u)(x_1, t) dt.$$

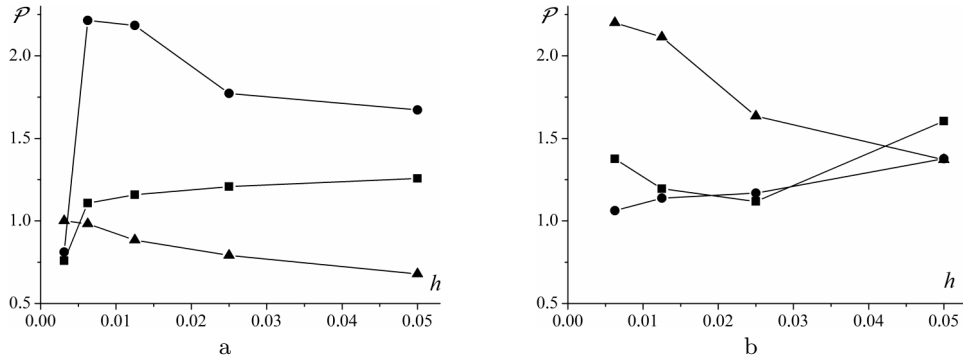


Figure 3. The rate of convergence of the density at different space steps, $\tau = 0.0005$, $t_2 = 0.4$, $t_1 = 0.3$, $x_1 = -0.6$, $x_2 = -0.2$: (a) calculation by the upwind scheme (the square symbol), with KCDS (the circle symbol), and with QGS (the triangle symbol); (b) calculation by the Steger–Warming scheme (the square symbol), with KCDS (the circle symbol), and with QGS (the triangle symbol)

On discontinuous solutions, plots of the approximation don't have the first order of accuracy [8]. The order of accuracy depends on the calculation domain. The definition of “accuracy order for discontinuous solutions” must be associated with the domain where these solutions are determined. The reason of the fractional order of restructuring of the conservation laws after restructuring the solutions is in the areas of collisions between the shock waves in the vicinity of the points where the new rarefaction wave has occurred [9].

Conclusion

The paper considered the derivation of equations with KCDS and QGS. This approach is used for the upwind-leap-frog and the Steger–Warming schemes. A number of tests for the Riemann problem on the condensing grids were performed. Comparison of results of the numerical experiments with the exact solution has shown the high accuracy of the upwind-leap-frog scheme for KCDS and QGS. Also, the advantages and disadvantages of KCDS and QGS were shown. A counterexample constructed with the use of the Steger–Warming scheme shows the necessity of considering the sequence of derivation of equations with KCDS and QGS.

References

- [1] Chetverushkin B.N. Kinetically-Coordinated Difference Schemes for Gas Dynamic. — Moscow: MSU, 1999 (In Russian).

- [2] Chetverushkin B.N., Elizarova T.G. Kinetic algorithms for calculating gas dynamic flows // *Zh. Vychisl. Mat. Mat. Fiz.* — 1985. — Vol. 25, No. 10. — P. 1526–1533 (In Russian).
- [3] Chetverushkin B.N., Romanyukha N.Yu. Kinetic and Lattice Boltzmann Schemes // *Parallel Computational Fluid Dynamics, Multidisciplinary Applications.* — Amsterdam: Elsevier, 2005. — P. 257–262.
- [4] D’Ascenzo N., Saveliev V.I., Chetverushkin B.N. On algorithm for solving parabolic and elliptic equations // *Zh. Vychisl. Mat. Mat. Fiz.* — 2015. — Vol. 55, No. 8. — P. 1320–1328 (In Russian).
- [5] Patankar S.V. *Numerical Heat Transfer and Fluid Flow.* — Taylor and Francis, 1980.
- [6] Steger J.L., Warming R.F. Fluxvector splitting of the inviscid gasdynamic equations with applications to finite difference schemes // *J. Comput. Phys.* — 1981. — Vol. 40. — P. 263–293.
- [7] Toro E.F. *Riemann Solvers and Numerical Methods for Fluid Dynamics.* — 2nd ed. — Springer, 1999.
- [8] Godunov S.K., Manuzina Yu.D., Nazarieva M.A. Experimental analysis of convergence of the numerical solution to a generalized solution in fluid dynamics // *J. Comput. Math. and Math. Phys.* — 2011. — Vol. 51, No. 1. — P. 88–95.
- [9] Godunov S.K., Kulikov I.M. Computation of discontinuous solutions of fluid dynamics equations with entropy nondecrease guarantee // *J. Comput. Math. and Math. Phys.* — 2014. — Vol. 54, No. 6. — P. 1012–1024.

